SCIENTIFIC COMMITTEE
TENTH REGULAR SESSION

Majuro, Republic of the Marshall Islands
6-14 August 2014

Project 62: Progress report on climate simulations

WCPFC-SC10-2014/EB-IP-02
Revision 1 23 July 2014

S. Nicol[1], M. Dessert[2], T. Gorgues[2], O. Aumont[2], C. Menkes[3], P. Lehodey[4], M. Lengaigne[5]

1. Oceanic Fisheries Programme, SPC, BPD5, 98848 Nouméa, New Caledonia.
2. IRD, LPO, Institut Universitaire Européen de la Mer - 29280 Plouzané France
3. IRD, LOCEAN, BP A5, 98848 Nouméa, New Caledonia
4. Marine Ecosystem Department, CLS, 31526 Ramonville St Agne Cedex, France
5. Laboratoire d'Océanographie et du Climat: Expérimentation et Approches Numériques (LOCEAN), 4 Place Jussieu, 75252 Paris Cedex 05, France

Key Issues for SC10

1. The SC10 notes the construction of new climate forcing data to forecast tuna distributions and abundance over the longer time frame.
2. The SC10 includes optimisation of SEAPODYM for the four tropical tuna with this new climate forcing in the future work plan of Project 62.
3. The SC notes that an additional ecosystem model for simulating climate effects on tuna, APECOSM-E has been developed and optimised for skipjack in the Indian Ocean. The optimisation of this model for skipjack in the Pacific Ocean would provide the SC with further additional advice on the impact of climate on skipjack in the WCPO. A brief summary of APECOSM-E is provided in this report.
4. The SC10 is requested to establish a new "no cost" project for APECOSM with the objectives of applying this model to tropical tunas in the WCPO to evaluate the combined impacts of climate and fishing. The project would report back to the SC at its annual meeting. Project implementation will proceed on the basis of third-party funding. There would be no financial implications for the SC or WCPFC.

Introduction

SEAPODYM is a model developed for investigating spatial tuna population dynamics, under the influence of both fishing and environmental effects. The model is based on advection-diffusion-reaction equations, and population dynamics (spawning, movement, mortality) are constrained by environmental data (temperature, currents, primary production and dissolved oxygen concentration) and simulated distribution of mid-trophic (micronektonic tuna forage) functional groups. The model simulates tuna age-structured populations with length and weight relationships obtained from independent studies. Different life stages are considered: larvae, juveniles and (immature and mature) adults. After their juvenile phase movement is linked to fish size and habitat in addition to transportation by oceanic currents. Fish are considered immature until a pre-defined age at first maturity and mature after this age (i.e., contributing to the spawning biomass). Mature fish displacement may also be controlled by a seasonal switch between feeding and spawning habitat. The last age class is a "plus class" where all oldest individuals are accumulated. The model includes a representation of fisheries and predicts total catch and size frequency of catch by fleet when fishing data (catch and effort) are available. A Maximum Likelihood Estimation approach is used to optimize the model parameters.

Development and application of the SEAPODYM model is included in the WCPFC Scientific Committee work program through Project 62.

SEAPODYM uses spatially explicit estimates of ocean and biological properties such as temperature, current speed, oxygen, and phytoplankton concentration from physical-biogeochemical ocean models to constrain tuna population dynamics. Physical-biogeochemical ocean models require certain inputs that describe the physical boundaries of their domain. This includes information on surface winds, heat and salt fluxes, as well as surface fluxes of various chemicals or nutrients (e.g. CO_2 or O_2). These values are derived from theory or from a combination of theory and direct observational data. The assimilation of observational data allows better parameterization of the model resulting in more realistic reconstructions of historical ocean conditions.

Forecasts, where the physical-biogeochemical ocean model attempts to predict the future evolution of oceanic properties, can span a range of time scales. Seasonal forecasting models attempt to simulate near-term natural variability whereas climate models attempt to simulate longer term changes in the mean state of the ocean. In both types, the models are initialized and then permitted to evolve freely to estimate how the ocean might develop over a number of months for seasonal forecasting or over 50 to 100 years for climate forecasting scenarios. The most advanced forecasting models assimilate past observational data to capture historical conditions during the initialization.

New Physical Forcing for Future Climate Scenarios

Coupled models commonly used for climate forecast simulations are known to display significant biases in the mean state as well as in the variability of the ocean. Biogeochemistry of the ocean magnifies those biases due to inherent non-linearity which increases uncertainty in model predictions. This uncertainty is compounded further by the use of different biogeochemical modules, whose complexity varies from simple nutrient restoring schemes to the explicit representation of several plankton functional types. As a consequence, the comparison of the predictions of these different coupled models is extremely challenging. Moreover only a few atmosphere-ocean models have been coupled with an ocean biogeochemical component and consequently the uncertainty in climate predictions may only be partially represented by the models available.

Coupling ocean biogeochemistry with atmosphere-ocean models is expensive as is the optimization of SEAPODYM to numerous physical forcings of future climate. A more pragmatic approach is to construct a single physical forcing of the historical period that represents an ensemble of the available climate models. SEAPODYM can then be optimized to this forcing which can then be used as the parameterizations for subsequent forecasts using each climate model. We apply this innovative method using the NEMO ocean model (Nucleus for European Modelling of the Ocean; version 3.5) forced with a mix of “realistic” atmospheric fields (provided by an improved ERA-interim reanalysis) and atmospheric trends extracted from coupled climate models for the RCP8.5 scenario (which corresponds to the A2 “business as usual” scenario used in previous SEAPODYM simulation of changed climate). We coupled NEMO to the biogeochemical model PISCES (Pelagic Interaction Scheme for Carbon and Ecosystem Studies, Aumont and Bopp, 2006) at a coarse horizontal resolution of 2° (ORCA2 grid with a refined resolution of 0.5° in the equatorial band) to keep simulation cost low as several runs of more than 100 years were required. With this method, we produce simulations of the dynamic and biogeochemical state of the ocean which span over the historical (1979-2010) and the future (2011-2100) periods. We restricted the numbers of climate coupled models that were used to build our forcing sets to those involved in the Coupled Model Intercomparison Project Phase 5 (CMIP5) that captured El Nino Southern Oscillation (ENSO) cycles in their simulation [Bellenger et al., 2013, Table 1].

Table 1: Atmospheric coupled models considered in the new seapodym forcing

Modeling Center	CMIP5 model name
IPSL	IPSL-CM5A-MR
GFDL	GFDL-ESM2G
NorESM	NorESM1-ME
MPI	MPI-ESM-MR
MIROC	MIROC-ESM

To capture interannual and decadal variability and trend in mean state we constructed two different sets of atmospheric forcing fields. In the first set, the low frequency trend from the coupled models was added to the full reanalysis product. The seasonal to decadal variability of this forcing dataset is fully constrained by the reanalysis and remains unchanged in the future. In the second set, anomalies have been constructed from each coupled models by subtracting the monthly climatologies computed over the historical period (1979-2010). These anomalies have then been added to a monthly climatology computed from the reanalysis. The mean state is constrained by the reanalysis whereas the short to long-term variability is derived from the coupled models and includes climate change impacts. These two sets of forcing fields were used to force NEMO coupled with the biogeochemical module PISCES.

The historical simulation was run using the Drakkar Forcing Sets 5.2 (DFS5.2) which is based on the ECMWF (European Centre for Medium-Range Weather Forecasts) reanalysis ERA-INTERIM (atmospheric temperature, zonal and meridionnal wind speeds, radiative heat fluxes, relative humidity, precipitation) which has been corrected using satellite data (SSMI for temperatures, Quikscat for wind, ISCCP for radiative fluxes, see Dussin et al., 2013 for a detailed description of the corrections). Therefore the historical simulation was restricted to the period of the ERA-INTERIM reanalysis from 1979 to 2011. Salinity, temperature and biogeochemical tracer concentrations (nitrate, phosphate, iron, silicate, alkalinity, dissolved oxygen and dissolved organic and inorganic carbon) were initialized from the World Ocean Atlas climatology (WOA09, [Antonov et al., 2010; Garcia et al., 2009]), and model climatologies for iron and dissolved organic carbon. To avoid any substantial numerical drift in the simulations related to a non-equilibrated initial state, we applied a spin-up of the ocean model for 66 years cycling twice over the DFS5.2 forcing sets.

During those 2 cycles, the Sea Surface Salinity (SSS) was damped toward the WOA09 values (through a freshwater correction of net precipitation vs. evaporation) to avoid strong biases relative to the observations. This restoration technique, while preventing the modeled salinity from drifting away from the observations, dampens the inter-annual to decadal variability and prevents any substantial long term change in salinity (e.g. as a consequence of future climate change). To avoid this problem we estimated a monthly climatology of the freshwater flux correction imposed by this restoring term from the second cycle of the model spin-up. This climatological flux correction was then applied to both historical and the future simulations. The change in the damping procedure induced a weak discontinuity in the model solution that was absorbed by spinning-up the model for another 11 years (i.e. 77 years of spin-up). During the third cycle a salinity damping term was only applied to under polar sea-ice to avoid excessive convection in the high latitudes. The fourth cycle (C4) was the reference historical simulation and spanned the period from 1979 to 2011. The same methods were applied to this cycle that was applied to the 3rd cycle. The estimates from the end of this cycle were used as the initial state for our simulations

in forecast mode.

We applied the same two methods as used for the historical simulation for including long term trend and seasonal, inter-annual and decennal variability into the future climate scenarios. To include low frequency trends on ocean biogeochemistry due to a warmer climate we initially smoothed outputs of the coupled models with a 31-year wide Hanning filter. The hanning filter removes years at the beginning and the end of a time series. We compensated for this loss by computing a spline which replicated the hanning filtered time series and inferred from this spline the pattern for the lost years. This spline was added to three cycle of 30 years of DFS5 forcing sets (after some interpolations in space and time to match the DFS5 file format). The results are 90 year forcing sets that span the period 2010-2100 and include non-altered DFS5 "realistic" variability with long term trends due to climate change (Figure 1). This first approach has been completed for the IPSL and GFDL models.

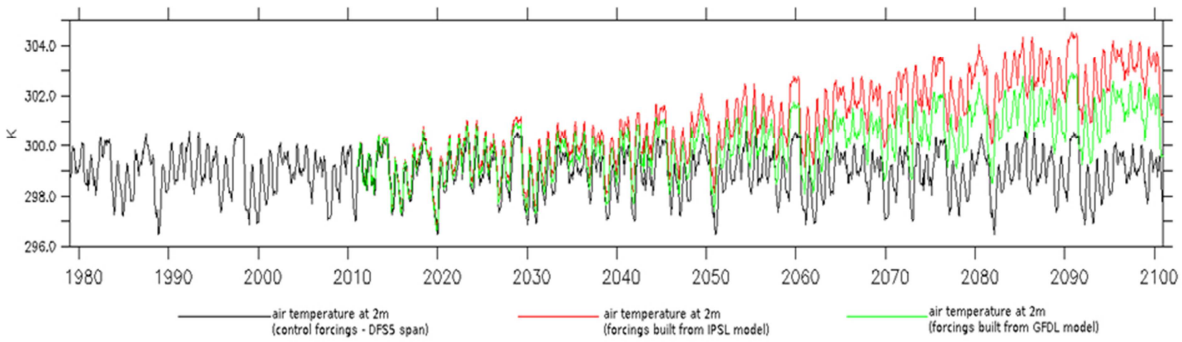

Figure 1 Time series of the air temperature at 2m (averaged over the nino3.4 box) for the DFS5.2 forcing set in Black, our forcing built following the 1st method using the ISPL coupled model outputs in red and our 1st method forcing using the GFDL outputs in green

The second method generated an adjusted DFS5.2 reanalysis. This was achieved by calculating a daily climatology for the period 1979 to 2010 from the DFS5.2 reanalysis. This removed the realistic seasonal, inter-annual and decadal variability of DFS5. Anomalies were then constructed from each of the coupled CMIP5 models by subtracting the monthly climatologies computed over the historical period (1979-2010). These anomalies were then added to the monthly climatology computed from the DFS5.2 reanalysis. This generated an alteration of the seasonal, inter-annual and decadal variability of DFS5 "realistic" climatology due to climate change. This second method has not yet been finalized for any of the selected climate models.

Prior to analyses of the simulations in forecast mode, we documented and validated the behavior of our model for the historical period. Figure 2 displays the globally averaged sea surface salinity, sea level and temperature for all the cycles prior to the simulations in forecast mode. During the spin-up period (C1+C2+C3), the model global trends are weak and acceptable. The sea level decreases by around 0.1 mm per century and salinity is constant. The global temperature shows a weak trend during the two first cycles and then increases by about 0.05°C during the last 44 years which corresponds to about 0.1°C/century.

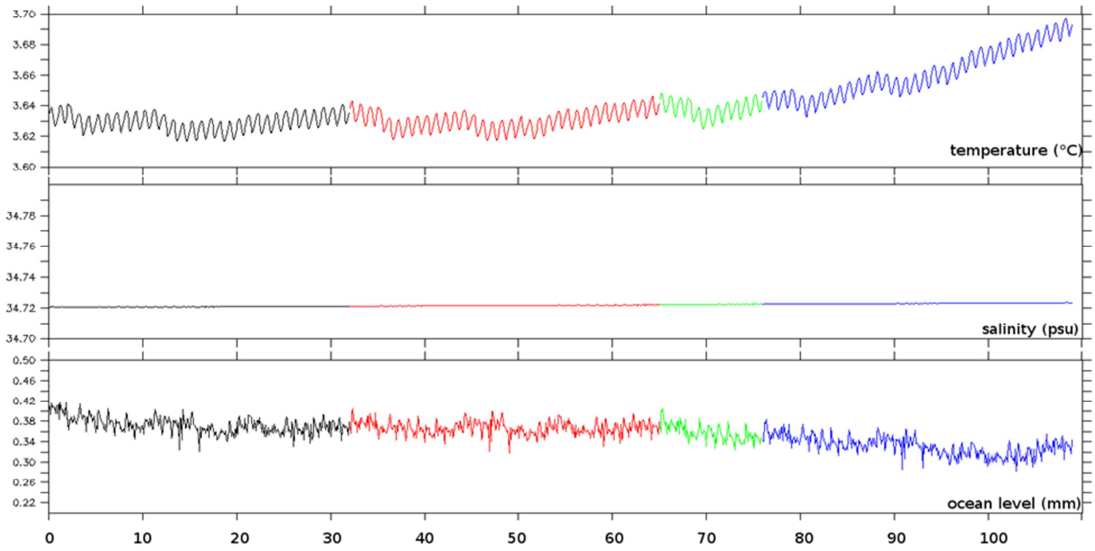

Figure 2: time series of globally averaged temperature (top panel), salinity (middle panel) and sea surface height (bottom panel). The years in the x-axis represent the total number of simulated years. Black and red parts of the plots indicate the spin-up period forced by 2 cycle of DFS5.2 forcing sets with the sea surface salinity damping (cycle 1 and 2). Green and Blue parts represent respectively the cycle 3 (11 years) and cycle 4 (our 1979-2010 reference historical period). The last two cycles (cycle 3 and 4) use the climatological sea surface salinity damping diagnosed from cycle 2 (refer to the text for details)

In comparison with observations, the surface temperature and salinity of the reference historical simulation approximate the data and spatially well-structured (Figure 3). However, noticeable biases are evident. These are commonly observed at the coarse resolution used in our study. The latitudinal position of the Kuroshio and the Gulf Stream currents, for example, are badly represented resulting in sea surface temperature and salinity biases noticeable in the North West Atlantic and Pacific Ocean. The solution given by our model in SST for the Southern Ocean seems also biased when compared to Levitus values. In the tropical Pacific SST and SSS did not display any redhibitory biases despite a cold bias of -1°C in the central equatorial zone (between 170°W and 100°W) and a warm bias of 1°C in the eastern part of the basin (90°W). The tropical Pacific was the least biased region of our historical simulation. A similar comparison using output from the IPSL coupled model for the historical period is shown in Figure 4 and comparison with Figure 4b demonstrates the reduced bias provided by our historical period.

Figure 5 represents the temporal variability of the surface temperature at the equator in the Pacific Ocean. Our simulation displays a cold bias when compared to satellite SST observations. Warm events in 1982-83 and 1998-99 both in the data and in the model correspond to El Nino events. Our historical simulation is therefore able to capture most of the seasonal and inter-annual variability of the eastern Pacific. The vertical dynamical features were also investigated to as the models ability to capture the characteristics of the Equatorial Under Current. Figure 6 shows that our model simulates a surface westward current of 30 to 40 cm/s all over the equatorial basin which is close to the observed values. In the sub-surface, a simulated Equatorial Undercurrent (EUC) flows eastward at 40 cm/s in the western

Pacific (~ 165°E) to 1 m/s at 80m deep in the eastern Pacific (~ 110 °W) which is coherent with observed values (Figure 5).

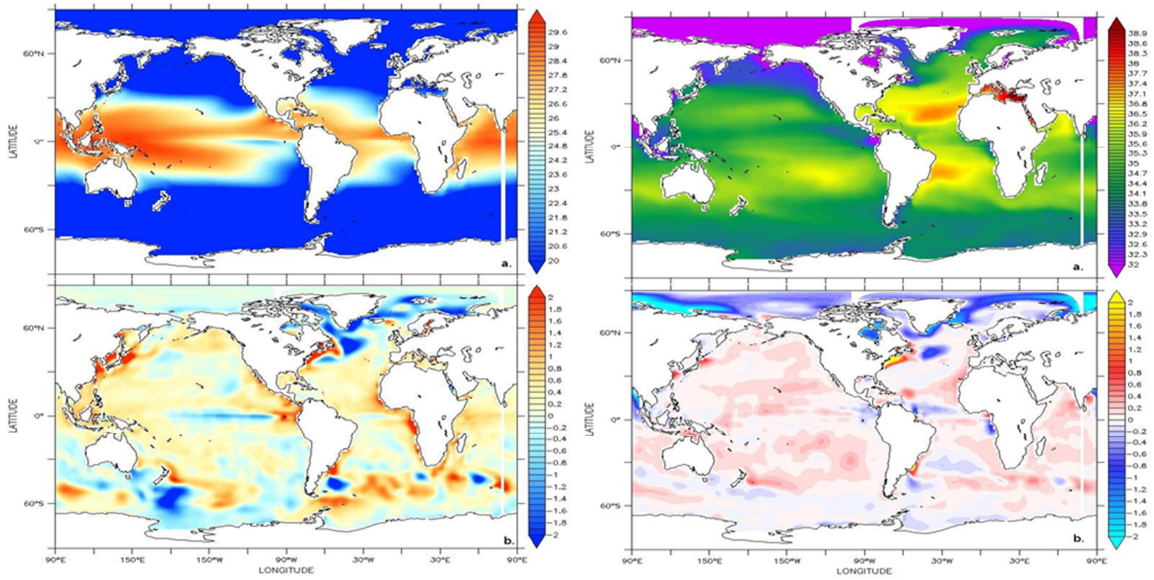

Figure 3: Global mean values of SST (respectively SSS) from our historical simulation outputs -C4- (A respectively C) and anomaly compared to SST climatology (SSS) from Levitus database (B respectively D).

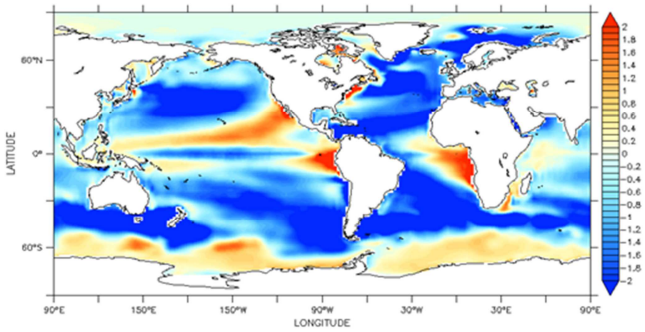

Figure 4: SST anomaly of the IPSL coupled model climatology on the historical period relative to the Levitus database climatology (same as figure 3B but for IPSL coupled model)

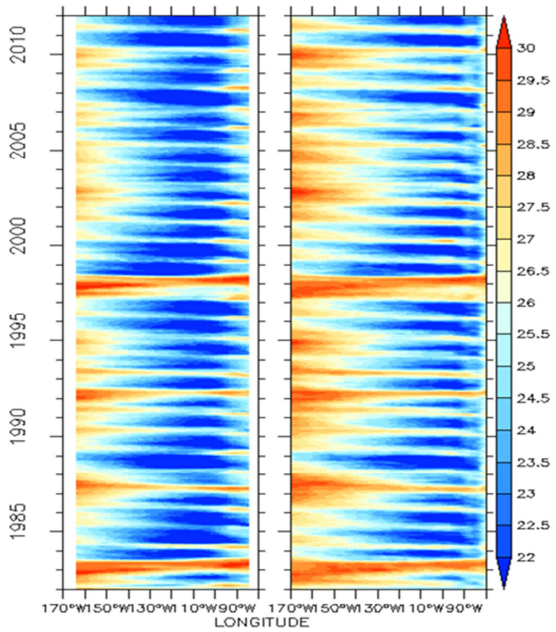

Figure 5: Hovmoller of surface temperature in Pacific equatorial ocean (0°N;170°W-80°W) from January 1981 to december 2011. Left: simulation outputs. Right: observations from AVHRR.

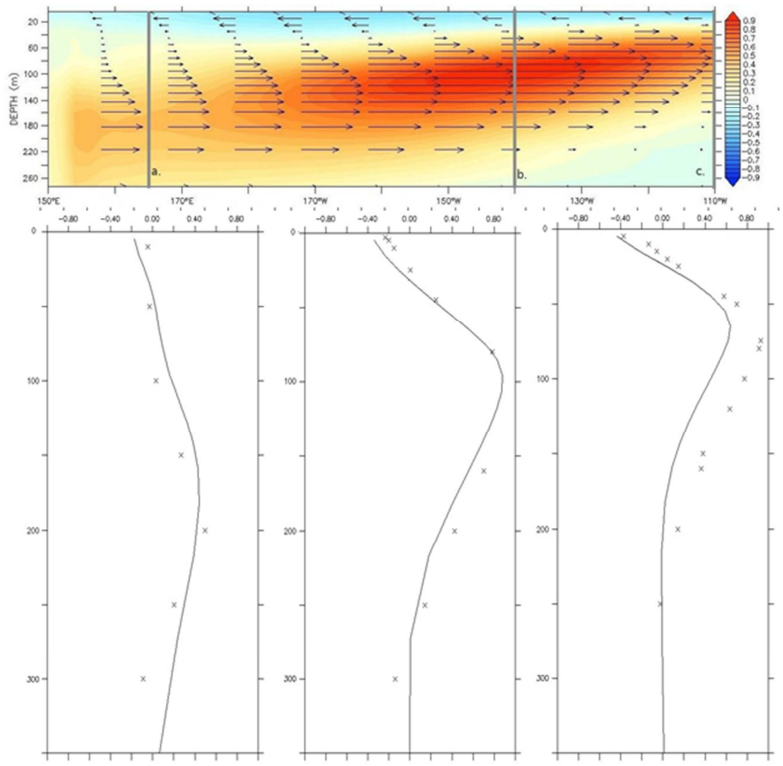

Figure 6: (top) Vertical equatorial section in Pacific ocean (from 150°E to 110°W at 0°N) of modeled mean zonal currents (m/s) ; (bottom) profiles of mean zonal currents (m/s) between 0,7°S and 0,7°N at 165°E (a.), 140°W (b.) and averaged between 100 and 100,5°W (c.), from TAO database for 1979-2011 period (stars symbol), for our modeled zonal current (black line).

In order to validate the biogeochemical component of our simulation, we compared our simulated chlorophyll with observed chlorophyll concentrations. Figure 7 shows that surface chlorophyll mean concentrations simulated by our model displays biases, mainly in the equatorial Atlantic, North West Pacific and Atlantic, and in the Southern Ocean. The discrepancies in the western parts of the North Atlantic and Pacific Oceans are probably related to the incorrect representation of the western boundary currents (Gulf Stream and Kuroshio currents). In the Southern Ocean, chlorophyll concentrations are significantly overestimated by the model. However, concentrations derived from satellite data are known to be significantly underestimated, by a factor of about 2, relative to in situ observations (Garcia et al., 2005, Kahru et al., 2010). Biases in the Arabian Sea are probably related to an insufficient horizontal resolution to properly reproduce the western boundary upwelling systems as well as the intense mesoscale activity observed in this region (Resplandy et al., 2011). Despite some local discrepancy between our simulation and satellite derived chlorophyll concentration around islands (ex : Galapagos) and near the American coast, our simulated mean equatorial Pacific Chlorophyll is close to the observed values.

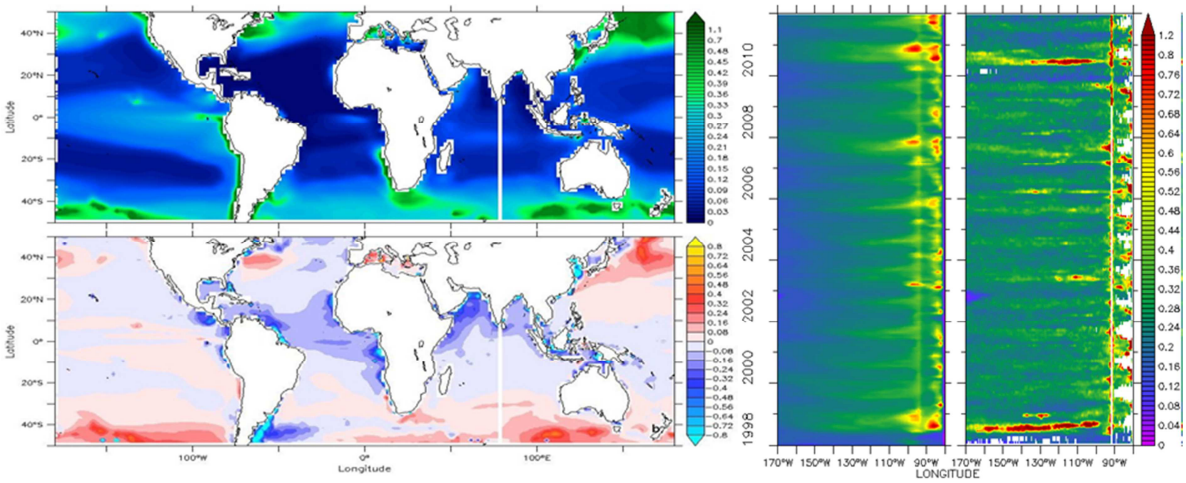

Figure 7: Global mean values of surface chlorophyll concentration from historical outputs -C4- (a.) and anomaly compared to mean global chlorophyll concentration from Seawifs database (b), between 50°S and 50°N (consistent with Seawifs satellite cover). Second panel shows hovmoller of surface chlorophyll concentration (mg/m3) of Pacific equatorial ocean (0°N ;170°W-80°W) from January 1998 to December 2011 : Left is the simulation outputs and right, the observations from Seawifs database.

At the equator, simulated blooms occur during La Nina events (Figure 7c and d) are consistent with Seawifs data. At the beginning of 1998, the surface chlorophyll concentration is weak (between 0.1 and 0.2 mg/m3) whereas it increases at the end of the year to values close to 1 mg/m3 in the Eastern Pacific. This increase is noticeable in observed surface chlorophyll concentrations and corresponds to an El Nino event followed by a La Nina event in 1998-99. Furthermore, at the end of 2010, surface chlorophyll concentrations raise to 0.8 mg/m3 in the Eastern part of the basin, consistent again with Seawifs data. Despite the ability of our model to simulate the surface chlorophyll inter-annual variability in the eastern Pacific, some biases remain. Mean chlorophyll values are underestimated by the model in the cold tongue and the blooms do not spread sufficiently westwards. It should be noted that tuning the biogeochemical model to better represent the inter-annual variability of the surface chlorophyll degrades the solution in term of mean surface chlorophyll and its seasonal variability.

Figure 8 compares modeled temperature, salinity, chlorophyll, iron and nitrate variability in the equatorial Pacific ocean and highlights the ENSO events during the whole simulated period (from 1979 to 2011). Surface nitrate concentrations are close to observed values from Levitus database, i.e. around 10 umol/L in winter in the eastern Pacific while concentrations range from 3 to 5 umol/L in the Western Pacific (not shown).

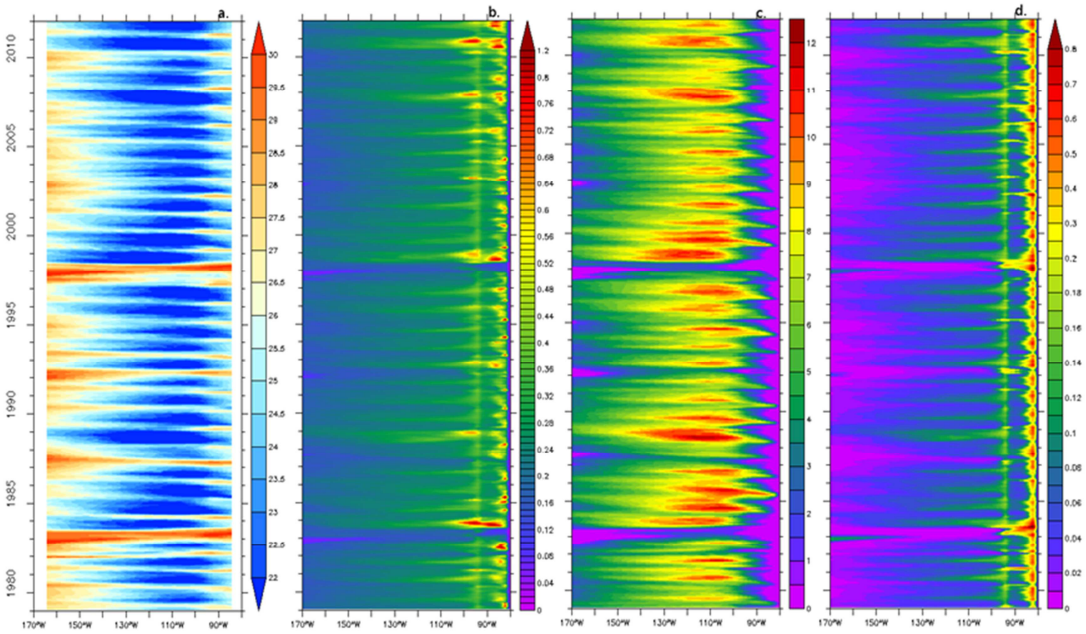

Figure 8: Hovmoller of simulated surface temperature (a.), chlorophyll concentration (mg/m3) (b.), nitrate concentrations (mmol/m3) (c.) and iron concentrations (nmol/m3) (d.) in the Pacific equatorial ocean (0°N ; 170°W-80°W) from January 1979 to December 2011.

Despite some dynamical biases (Gulf Stream, Kuroshio, and Southern Ocean) which are common in model with coarse resolution, our historical simulation was able to capture the main structures of the mean state and the variability of the tropical Pacific. Although blooms intensity is not sufficiently strong during La Nina events, inter-annual variability was reasonably well represented by the model.

Ocean Future Simulations

The inclusion of long term trend into the future climate scenarios has been completed for the IPSL and GFDL models, however validation of these simulations has only just commenced for the IPSL test case. A comparison between our simulation and the IPSL simulation shows:

(1) Similar large scale patterns of SST warming (Figure 9). However, there are some differences. The most prominent examples are the differences in the Southern Ocean and in the equatorial upwelling. For the latter, the lower amplitude of the SST warming in our simulation could be explained by a more intense equatorial upwelling in our simulation due to more energetic wind stresses in the equatorial band. The second difference (i.e. the cooling in the Southern Ocean) is due to a mismatch between the trends computed from the coupled model and the spatial patterns of our forced simulation. Figure 10 shows that the climatic trends of the meridional component of the surface wind is acting on a stronger SST meridional gradient at the Antarctic front, leading to a significant difference between the IPSL model and our model simulations in

that region.

(2) Early results of surface Chlorophyll comparison (Figure 11) shows similar patterns with some noticeable differences in the high latitudes and in the Pacific equatorial band. The latter is probably due our stronger equatorial upwelling.

(3) Completion of simulations for all five CMIP5 models is expected before December 2014 simulations incorporating seasonal, interannual and decadal variability.

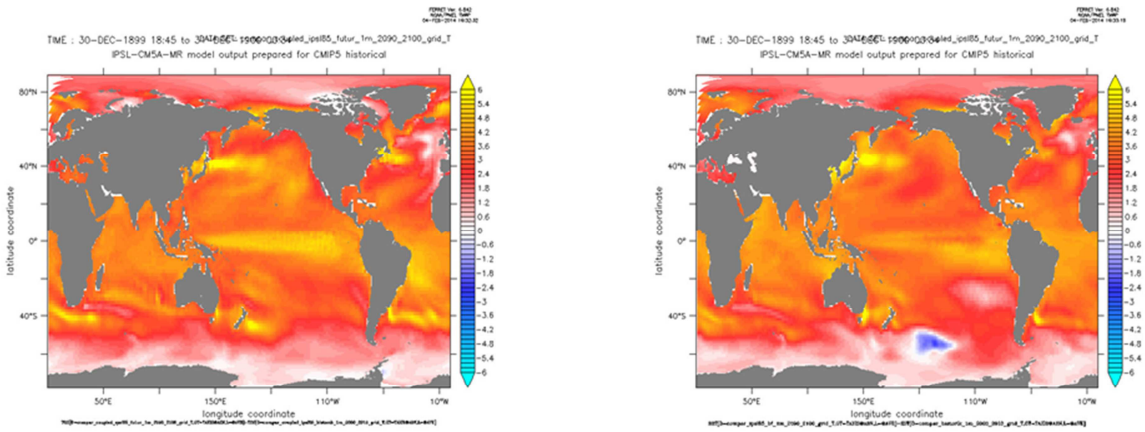

Figure 9: SST difference future (i.e. climatology 2090/2100)-past (i.e. clim2000/2010) for the IPSL coupled model (A). (B) same as (A) but using our simulation outputs instead of IPSL ones.

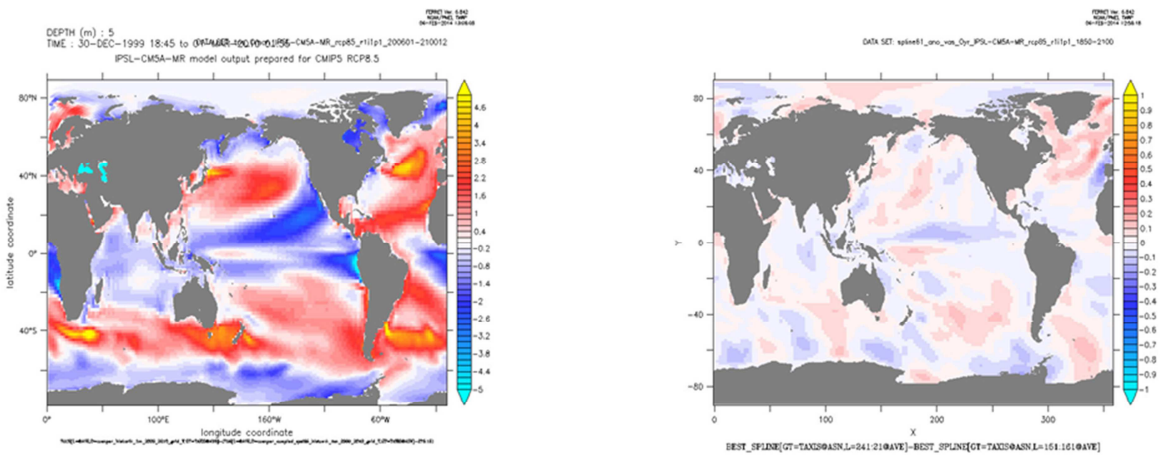

Figure 10: (A) SST difference between our historical simulation (DFS5 from 2000 to 2010) with the IPSL coupled model and (B) temporal trend of the meridional wind speeds between the historical and future periods.

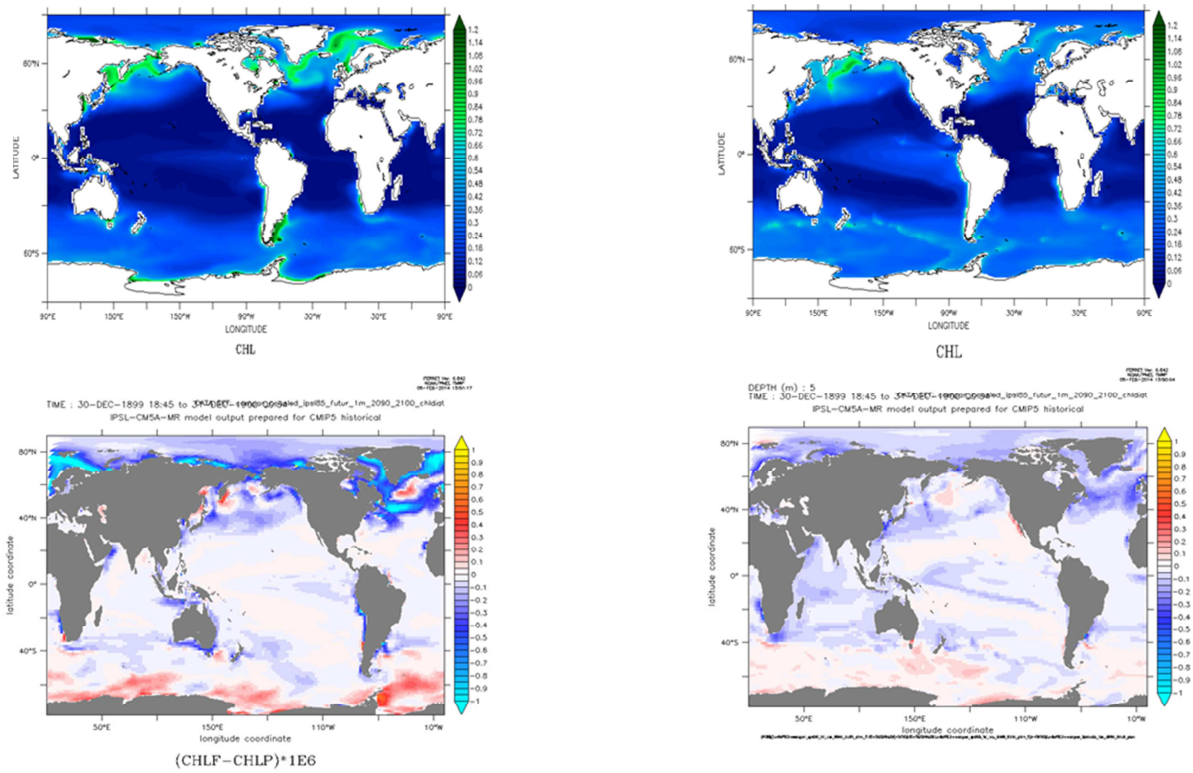

Figure 11: (A) Surface Chl concentration averaged over the 2000-2010 period from the fully coupled IPSL model. (B) same as A but for our historical simulation (2000-2010 period from our cycle 4). (C) difference for the IPSL coupled model (future-present) and (D) Same as A but for our DFS5 simulation.

APECOSM-E

APECOSM-E (Apex-Predator-Ecosystem-Model – Estimation) is a deterministic model that represents the 3D dynamic distribution of tropical tuna under the joint effect of environmental conditions and exploitation by fisheries. It is a simplified version of the top predator component of the APECOSM framework, based on a single partial differential equation. The model is structured in 3D space and fish weight (or size) and considers size dependent reproduction, growth, predation, natural mortality and fishing mortality. The representation of growth, reproduction and ageing mortality follows the dynamic energy budget theory, while horizontal movements and vertical distribution are driven by habitat gradients, physical currents and diffusion. Processes are time, space and size-dependent and linked to the environment through mechanistic bioenergetic or behavioural parameterizations.

The data assimilation algorithm used is based on the minimization of a Bayesian cost function that combines three terms: the distance between the computed and the observed catches in weight, the distance between the computed and the observed length frequencies and the prior density function of the parameters. The observation errors in catch data are assumed to follow a log-normal distribution, while the observation errors for length frequency are supposed to follow a normal distribution. The minimization of the cost function is calculated by minimizing the negative log-likelihood of the data plus

the negative log of prior density function.

APECOSM-E has been successfully parameterized for skipjack tuna in the Indian Ocean (Dueri et al. 2012a, Dueri et al. 2012b) and for evaluating global effects of future climate scenarios on skipjack using the Indian Ocean parameterisation (Dueri et al. 2014). Although similar in purpose and structure APECOSM-E differs from SEAPODYM by implementation of a mechanistic link between environmental factors, metabolic rates, and behavioral responses based on the dynamic energy budget theory. It also structures the vertical layers of habitat differently to SEAPODYM. It therefore provides an alternative model for exploring the interaction between tuna and climate.

Acknowledgements and Donors

S. Nicol, C. Menkes and P. Lehodey designed the project to construct a new physical forcing for climate simulations using SEAPODYM. M. Dessert, T. Gorgues, O. Aumont and C. Menkes implemented the project to build this physical forcing. S. Nicol and P. Lehodey are optimising SEAPODYM using this forcing. O. Maury and S. Dueri have developed the APECOSM project. The evaluation of future climate scenarios is currently supported by Secretariat of the Pacific Community, Collecte Localisation Satellites, Institut de Recherche pour le Développement with financial assistance from Australian Government Overseas Aid Program (AUSAID), 10th European Development Fund (EDF), Deutsche Gesellschaft für Internationale Zusammenarbeit (GIZ). The Inter American Tropical Tuna Commission has provided access to non-public domain data for the purposes of implementing the work programme of the WCPFC-SC.

References

Antonov, J. I., D. Seidov, T. P. Boyer, R. A. Locarnini, A. V. Mishonov, H. E. Garcia, O. K. Baranova, M. M. Zweng, and D. R. Johnson, 2010. World Ocean Atlas 2009, Volume 2: Salinity. S. Levitus, Ed. NOAA Atlas NESDIS 69, U.S. Government Printing Office, Washington, D.C., 184 pp.

Aumont, O. and L. Bopp, 2006 Globalizing results from ocean in situ iron fertilization studies, Glob. Biogeochem. Cy., 20, GB2017, doi:10.1029/2005GB002591, 2006.

Bellenger, H., E. Guilyardi, J. Leloup, M. Lengaigne, J. Vialard, 2013. Climate Dynamics:ENSO representation in climate models : from CMIP3 to CMIP5

Dueri, S., B. Faugeras, O. Maury. 2012a. Modelling the skipjack tuna dynamics in the Indian Ocean with APECOSM-E: Part 1. Model formulation. Ecological Modelling 245:41-54.

Dueri, S., B. Faugeras, O. Maury. 2012b. Modelling the skipjack tuna dynamics in the Indian Ocean with APECOSM-E – Part 2: Parameter estimation and sensitivity analysis. Ecological Modelling 245:55-64.

Dueri, S., L. Bopp, O. Maury. 2014. Projecting the impacts of climate change on skipjack tuna abundance and spatial distribution. Global Change Biology 20: 742–753.

Dussin R. and Barnier B., 2013: The making of DFS5.1. Drakkar project report. 40 p. LGGE, Grenoble, France.

Locarnini, R. A., A. V. Mishonov, J. I. Antonov, T. P. Boyer, H. E. Garcia, O. K. Baranova, M. M. Zweng, and D. R. Johnson, 2010. World Ocean Atlas 2009, Volume 1: Temperature. S. Levitus, Ed. NOAA Atlas NESDIS 68, U.S. Government Printing Office, Washington, D.C., 184 pp.

Garcia, H. E., R. A. Locarnini, T. P. Boyer, J. I. Antonov, O. K. Baranova, M. M. Zweng, and D. R. Johnson, 2010. World Ocean Atlas 2009, Volume 3: Dissolved Oxygen, Apparent Oxygen Utilization, and Oxygen Saturation. S. Levitus, Ed. NOAA Atlas NESDIS 70, U.S. Government Printing Office, Washington, D.C., 344 pp.

Garcia, H. E., R. A. Locarnini, T. P. Boyer, J. I. Antonov, M. M. Zweng, O. K. Baranova, and D. R. Johnson, 2010. World Ocean Atlas 2009, Volume 4: Nutrients (phosphate, nitrate, silicate). S. Levitus, Ed. NOAA Atlas NESDIS 71, U.S. Government Printing Office, Washington, D.C., 398 pp.

Garcia, C.A.E., V.M.T. Garcia, C.R. McClain. 2005. Evaluation of SeaWiFS chlorophyll algorithms in the Southwestern Atlantic and Southern Oceans. Remote Sensing of Environment, 95:125–137.

Kahru, M. S. T. Gille, R. Murtugudde, P. G. Strutton, M. Manzano-Sarabia,H. Wang, and B. G. Mitchell. 2010. Global correlations between winds and ocean chlorophyll. Journal of Geophysical Research, 115: C12040, doi:10.1029/2010JC006500

Resplandy, L., M. Lévy, G. Madec, S. Pous, O. Aumont and D. Kumar. 2011. Contribution of mesoscale processes to nutrient budgets in the Arabian Sea, Journal of Geophysical Research 116: C11007.